PHYSICAL REVIEW B **92**, 140505(R) (2015)

Thermally activated and quantum plasticity of solid ^{3}He at temperatures below 0.5 K

A. Lisunov,* V. Maidanov, V. Rubanskyi, S. Rubets, E. Rudavskii, S. Smirnov, and V. Zhuchkov
B.Verkin Institute for Low Temperature Physics and Engineering of the National Academy of Sciences of Ukraine, Kharkov 61103, Ukraine
(Received 19 June 2015; revised manuscript received 30 September 2015; published 22 October 2015)

Plastic flow of solid ^{3}He through a porous membrane frozen in the crystal is observed in the temperature range from 0.1 to 0.5 K. The flow of helium through the pores of the membrane occurs under the mechanical stress caused by the electrostatic force. It was found that the temperature dependence of the flow velocity V has two characteristic regions: at temperatures above $T \sim 0.2$ K, V decreases exponentially with lowering temperature, which corresponds to the thermally activated process, and at temperatures below 0.2 K, V is independent on T, which indicates the quantum mechanism of mass transfer. For the high-temperature region the values of thermal activation volume and energy of activation are estimated. The results are analyzed in the framework of vacancy and dislocation models of plastic flow.

DOI: 10.1103/PhysRevB.92.140505 PACS number(s): 67.80.D−, 62.20.fq, 62.20.Hg

Interest in the elastic and plastic properties of solid helium has strongly increased in recent years in connection with the anomalous behavior of solid ^{4}He at temperatures below 0.3 K. In particular, the change in the period of torsional oscillations [1] and a sharp change in viscoelastic properties [2,3] were observed. Currently, most of the authors came to the consensus that the detected anomalies have nonsuperfluid origin, and the key to understanding these anomalies is connected with the features of plasticity in helium crystals at low temperatures [4–6].

Torsion experiments and measurements of the shear modulus were carried out also in solid ^{3}He [6,7]. It has been found that in hexagonal-close-packed (hcp) phase anomalies observed are the same as in the ^{4}He, and in body-centered-cubic (bcc) phase they are absent. Such behavior only increased interest in the plastic properties of the solid ^{3}He.

The first experimental study of the plasticity of solid ^{3}He was performed in 1979 by examining the movement of a special brass rod frozen in the crystal [8]. The authors observed the plastic flow of bcc ^{3}He in the temperature range 0.5–1.0 K and explained it in the framework of the dislocation model. In the next series of experiments in 1993–1995 the plastic properties of solid ^{3}He were investigated by overflowing solid helium through a porous membrane in the same temperature range [9,10]. The results were described as vacancy diffusion flow.

Note that it seems rather actual to know in more detail the similarities and differences in plastic properties of solid ^{3}He and solid ^{4}He [11]. These quantum crystals follow different types of quantum statistics and have different amplitudes of zero-point vibrations. We can therefore expect that the dislocations and vacancies in such crystals have different characteristics, which results in a different nature of the plastic flow, especially at very low temperatures. An investigation of the plastic flow of solid ^{4}He under the same conditions was carried out by the authors earlier [12].

One of the present works is to find out the new features of the plastic properties of solid ^{3}He. A study of the plasticity of the crystals was carried out at temperatures below ∼0.5 K, where one can expect a clear manifestation of quantum effects. Another aim is to identify the carriers of mass transfer and mechanisms of plastic deformation in the solid helium in a wide range of temperatures and external loads.

The plastic flow of solid ^{3}He occurs as a result of constant stress due to displacement of the porous membrane frozen into a crystal. The measurement method was the same as that in similar experiments with solid ^{4}He [12]. The measuring cell (Fig. 1) consisted of two chambers I and II with solid helium separated by a porous membrane which is made of a metallized polymer film. The membrane had a radius of 10 mm and a thickness of 10 μm, the orifice diameter was 6–8 μm, and a porosity of 0.18. Chamber I forms a parallel-plate capacitor consisting of a fixed electrode and the membrane which served as a movable electrode. The distance between the electrodes of the capacitor was ∼25 μm, and the height of chamber II was 2 mm.

Initially, the electrical potential difference across the electrodes of the measuring capacitor was zero, and the membrane had a flat shape being parallel to the fixed electrode. When we applied potential difference U to the electrodes of the capacitor, the force started to act on the membrane. As a result, the following compression mechanical stress σ appears in solid helium:

$$\sigma = \frac{2\pi C^2 U^2}{\varepsilon S^2}. \quad (1)$$

Here C is the capacitance of the measuring capacitor, S is the membrane area, U is the potential difference, and $\varepsilon \approx 1$ is the dielectric constant of solid ^{3}He. Solid helium under stress flows through the orifices in the membrane, which connected chamber I and chamber II. This leads to a shift of the membrane, which is measured by the change in capacitance. Thus, the recorded time dependence of C allowed one to find the average velocity of the membrane corresponding to the velocity of helium:

$$V(t) = \frac{\varepsilon S}{4\pi C^2}\frac{dC}{dt}. \quad (2)$$

Velocities were found at different temperatures and stresses.

^{3}He under investigation previously was subjected to distillation from impurities of ^{4}He by rectification in a special open column; the possible concentration of ^{4}He was less

*lisunov@ilt.kharkov.ua

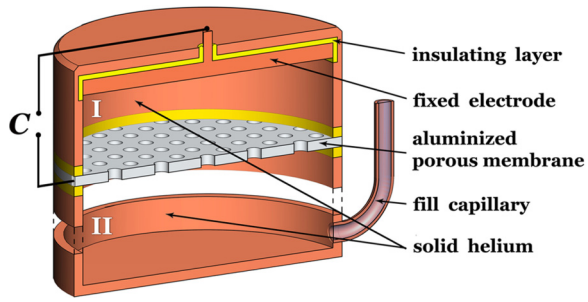

FIG. 1. (Color online) The design scheme of the measuring cell. It is shown not to scale.

than 10^{-5}. The cell temperature was determined using a film resistance RuO_2 thermometer calibrated by a ^{3}He melting curve thermometer.

Eleven samples of ^{3}He in the bcc phase have been studied, that were grown by the capillary blocking at several molar volumes V_m from 22.96 to 24.43 cm^3/mole. The blocking capillary was fulfilled at temperatures above 1.5 K, and the next cooling down was realized with velocity 25 mK/min during 40 minutes until full crystallization of the sample was achieved. Measurements were carried out in such as-grown crystals from low temperatures up to the premelting area where the rate of plastic flow increased by orders of magnitude and the position of the membrane deviated considerably from the equilibrium position. To return the membrane to its original position, the crystal was remelted under blocked capillary, i.e., at the same density as the crystal. The sample pressure was controlled by the capacitance sensor, and the equilibrium position of the membrane was determined by the capacitance of the measuring capacitor. The defect structure of the samples was not controlled specially.

Figure 2 shows the primary experimental data describing the change in the capacitance of the measuring capacitor after application of the electric force to the plates (creep curves). This was accompanied by a flow of solid helium through the orifices in the membrane; the capacitor gap was decreased in the measurement capacitor, and its capacity was increased. Note that at zero voltage ($U = 0$ and, consequently, $\sigma = 0$) the capacity of the measuring capacitor $C \approx 100$ pF did not change over time with an accuracy of 10^{-4} pF, indicating the absence of macroscopic plastic flow in solid ^{3}He at $\sigma = 0$. The dependencies of Fig. 2 correspond to the creep, when the capacitance C varies linearly with time. Despite the scatter of the experimental data, the results obtained can be approximated by straight lines whose slope dC/dt, in accordance with Eq. (2), allows us to find the average velocity V, which characterizes the overflow of helium. Measurements of the velocity V were performed at constant temperature and constant applied voltage U. After measuring the steady-state value of dC/dt the voltage U was changed to the new constant value, and the velocity measurement was repeated with the new values of U. Investigations were carried out at U values corresponding to the mechanical stress σ from 0 to 6×10^4 dyn/cm^2.

Figure 3 shows a typical inverse temperature dependence of the flow velocity of solid helium. It clearly shows the presence of two areas with different temperature dependence of the

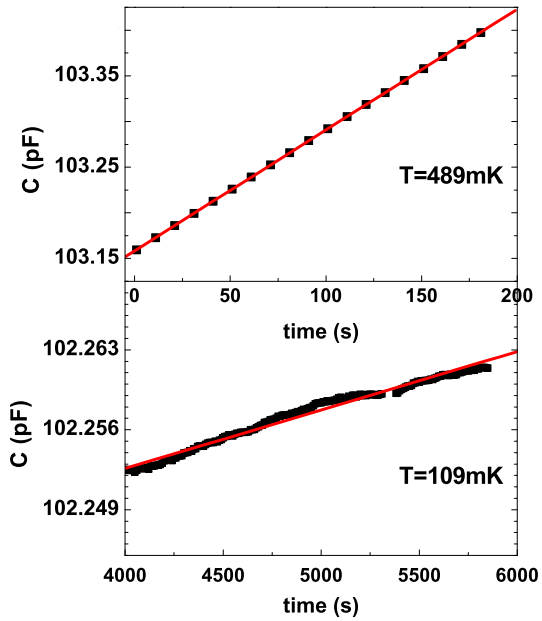

FIG. 2. (Color online) Typical creep curves of solid ^{3}He for one of the samples with $V_m = 24.43$ cm^3/mole for two different temperatures. The solid lines are a linear fitting of the primary experimental data. The applied voltage $U = 1000$ V.

velocity: at temperatures above $\sim$0.2 K the helium flow velocity decreases exponentially with lowering temperature, which is typical for a thermally activated process. At $T < 0.2$ K helium flow velocity is almost independent on temperature, which can be treated as a manifestation of the quantum tunneling mechanism of mass transfer. In this temperature area there is a large scatter of experimental data, and the area itself was revealed reliably only under sufficiently high stresses σ. Note that the measured velocity values depend on the defect structure of the sample. In a more dense crystal transition from the thermally activated to quantum region occurs at a lower temperature and shows lower flow rate values. In one of the studied samples the quantum region was not detected. We emphasize, that unlike ^{3}He, in solid ^{4}He the plastic flow does not have a quantum area [12]. However, the character of plastic flow in ^{4}He changes essentially with decreasing temperature.

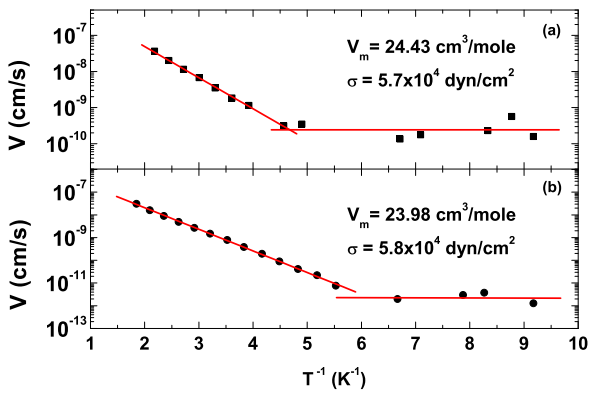

FIG. 3. (Color online) Temperature dependence of the flow velocity for two samples with different molar volumes and stresses.

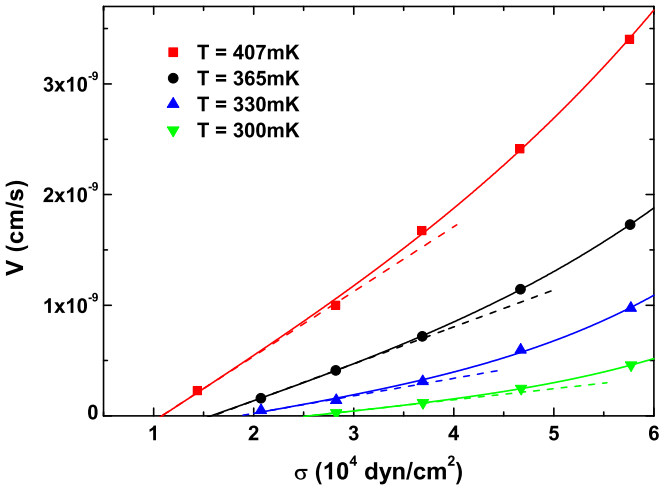

FIG. 4. (Color online) The stress dependence of the velocity of plastic flow at a constant temperature. Solid lines are approximations by expression (3). The dashed lines in all cases represent a linear stress dependence.

The dependencies of the flow velocity of solid helium on the stress in the thermal activation area are shown in Fig. 4. We did not observe the plastic flow at $\sigma = 0$, whereas $dC/dt \neq 0$ under increasing σ. Note that, first, at all temperatures the dependencies $V(\sigma)$ have a nonlinear segment. Secondly, one observes large scatter of dC/dt, while σ attains a certain value, which may be treated as the threshold stress which depends on temperature. The dependencies $V(\sigma)$ were registered reliably at stresses higher than those of the threshold value.

The analysis showed that the dependencies $V(\sigma)$ of Fig. 4 for fixed temperature may be approximated by the expressions (see Ref. [13], Chap. 16)

$$V(\sigma) = \tilde{V} \sinh\left[\frac{\gamma}{k_B T}(\sigma - \sigma_i)\right], \tag{3}$$

$$\tilde{V} = V_0 \exp\left(-\frac{E_a}{k_B T}\right), \tag{4}$$

where V_0 is the constant depending on the quality of the crystal; E_a and γ are activation energy and volume, respectively; σ_i is the internal threshold stress; and k_B is the Boltzmann constant. The approximation of the experimental data by Eqs. (3) and (4), made by the least-square method, is shown by solid lines in Fig. 4. Note that Eq. (3) gives linear dependence if $\gamma(\sigma - \sigma_i)/kT \ll 1$. The linear segments are shown in Fig. 4 by dashed lines. In opposite limit $\gamma(\sigma - \sigma_i)/kT > 1$ one has the exponential dependence on σ-σ_i: $V \sim \exp[\frac{\gamma}{k_B T}(\sigma - \sigma_i)]$. As is seen in Fig. 4, the range of measured experimental values of V contains both of these dependencies. Thus we obtained the values of the three empirical parameters: γ, σ_i, and $\tilde{V}$. It was found that the activation volume γ within the scatter of data is independent of temperature and is about 30–70 times the volume per one atom V_a (Table I). This table also contains the values of these empirical parameters obtained for five samples which were studied at various σ. The rest of the samples were studied at one value of σ.

As for the parameter $\tilde{V}$, the dependence of $\tilde{V}$ vs T^{-1} is well described by linear functions (Fig. 5), which corresponds to

TABLE I. The main characteristics of the studied samples in the thermally activated region.

Sample number	Sample type	V_m (cm^3/mole)	E_a (K)	γ/V_a	σ_i (10^4dyn/cm^2)
1	As-grown	22.96	2.85 ± 0.02	48 ± 5	0.60 ± 0.02
2	As-grown	23.71	3.11 ± 0.01	55 ± 20	2.26 ± 1.18
3	As-grown	23.98	3.06 ± 0.01	51 ± 17	1.79 ± 0.31
4	As-grown	24.25	2.36 ± 0.04	39 ± 8	1.09 ± 0.85
5	Remelted	24.43	2.79 ± 0.04	61 ± 15	1.82 ± 1.13

Eq. (4), where the parameter V_0 is independent of temperature, whereas dependent on the defect structure of the samples. According to Eq. (4), plotting dependencies $\ln\tilde{V}$ vs $1/T$ one can determine the activation energy E_a of plastic flow. The obtained values of the activation energy are $E_a = 2.32$–3.07 K in the studied range of the molar volume V_m (Table I). These values are in good agreement with the data on the activation energy of vacancies in solid ^{3}He obtained in x-ray experiments [14] made under conditions where there is no directional movement of vacancies. This agreement means that, whereas the formation of vacancies is the thermally activated process, their movement in the crystal ^{3}He occurs due to quantum tunneling.

At the same time there is a contradiction with the usual vacancy model. On the one hand, the values obtained for the activation energy of the process are in agreement with the vacancy mechanism; on the other hand, large values of the activation volume γ mean that the process of plastic deformation causes a change in the lattice in a scale considerably exceeding the atomic size V_a.

In such a situation one can assume that the vacancy diffusion mechanism of a plastic flow in solid helium is provided by the vacancy sources which are areas with a high concentration of external stresses. In this case, usually stress concentration factor α_k is introduced, which shows that the value of the mechanical stress σ can reach $\alpha_k\sigma$ in a stress concentration

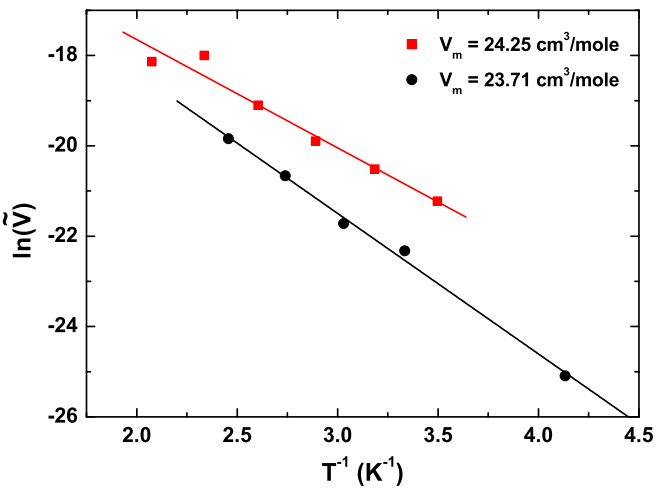

FIG. 5. (Color online) Dependencies of $\ln\tilde{V}$ vs $1/T$ and their approximation by linear functions for two samples with different molar volumes.

area [15]. These areas in the used cell are supposed to be areas near the orifices in the membrane and other inhomogeneous areas. Thus the value of $\alpha_k V_a$ has a sense of measured activation volume. As shown in Refs. [16,17], the value of α_k may vary in a wide range attaining a value of 40, which gives $\alpha_k V_a \approx 40 V_a$ in good agreement with the value of γ, found from the above experimental data. Note also that the high value of the parameter α_k leads to a nonlinear dependence of the velocity of diffusion flow on the external stress under attainable load in the experiment. It is just that dependence $V(\sigma)$ given by Eq. (3) is observed experimentally (see Fig. 4).

An alternative to the proposed vacancy mechanism is dislocation mechanisms associated with the motion of dislocations through local barriers. Using empirical values of γ, we have made, according to Refs. [13] and [18], the standard estimation of the average area per one local barrier, the average density of the forest dislocations, and the value of the internal stress caused by them. Estimates have shown that the average area per one local barrier is $(2–14) \times 10^3 a^2$, where a is lattice parameter. The local barriers may be either the impurity atoms of ^{4}He in crystals of ^{3}He or forest dislocations. However, the estimates show that the concentration of ^{4}He in ^{3}He samples is more than one order less than that sufficient to form the necessary number of local barriers. As for the forest dislocations (dislocations crossing the slip plane of the moving dislocation), estimates have shown that for the interpretation of experimental data, the density of the forest dislocation should be $\approx 10^{14}$–10^{15} m^{-2}. However, such a density of forest dislocations should create long-range internal stresses in the crystal which are two orders of magnitude higher than the maximum stress σ in this experiment. This contradiction does not allow one to accept the assumption that the forest dislocations are barriers that control the process of plastic flow.

The dislocation model of plastic flow can adequately describe the results obtained in this experiment, if we consider the dislocation motion in the Peierls potential relief, the theory of which was developed in Refs. [19–23]. Such approach has allowed one to identify the mechanisms of dislocation motion in the Peierls relief in a series of materials [24–28]. In this case the dislocation motion provides the formation and the further expansion of kink pairs, and the rate of plastic deformation $\dot{\varepsilon}$, which, being proportional to the measured macroscopic flow velocity $V(T,\sigma)$ of ^{3}He, is determined by the probability of nucleation of kink pairs w_T and further their dynamic expansion.

The probability w_T is determined by the energy $H(\tau^*)$ of nucleation of critical kink pair on a dislocation which is dependent on the effective shear stress $\tau^* = \tau - \tau_i$ (τ is the external applied stress; τ_i is the internal stress). In the wide range of stresses τ^* the expression for w_T can be written [21,22,24,25,28]

$$w_T \propto \exp\left(-\frac{H(\tau^*)}{k_B T}\right) = \exp\left(-\frac{H^* - E(\tau^*)}{k_B T}\right), \quad (5)$$

where H^* is the energy parameter and $E(\tau^*)$ is a complicated function of τ^*.

For a comparison between experiment and theory one applies Eqs. (3) and (4) for the experimentally measured velocity V, which under condition $\gamma(\sigma - \sigma_i)/k_B T > 1$ reads as

$$V(\sigma,T) \approx \frac{V_0}{2} \exp\left(-\frac{E_a - \gamma(\sigma - \sigma_i)}{k_B T}\right). \quad (6)$$

A connection between strain rate $\dot{\varepsilon}$ and the probability w_T is known in two limiting cases: low and high linear density of kinks [21]. In the limit of low density the value $\dot{\varepsilon}$ is determined by the average time of nucleation of kink pairs and $\dot{\varepsilon} \propto w_T$, whereas $H^* = 2W_k$ where W_k is the energy of a single kink on a dislocation. To adequately describe the experimental data on the velocity of plastic flow of ^{3}He, one should suppose the consistency between the exponents of Eqs. (5) and (6), because $\dot{\varepsilon} \propto w_T$. Therefore one should put $H^* = E_a$ and, hence, $W_k = E_a/2$. Assuming that the Peierls relief is sinusoidal, it can find, according to Refs. [13] and [19], the width of a single kink l_k and evaluate Peierls stress τ_P. Estimates show that the value of l_k is about six times periods a_P of the Peierls potential. This means that a single kink is extensive and allows one to apply the continual model of dislocation. The value of the Peierls stress is estimated as $\tau_P = (1–1.8) \times 10^6$ dyn/cm^2, which is two orders of magnitude higher than stresses in our experiment, that is, $\tau^* \ll \tau_P$. Under these conditions, an estimate of the activation volume gives $\approx(16–30)V_a$, which is consistent with the values obtained for empirical parameter γ.

If the linear density of kinks is high, the processes of their annihilation are essential and $\dot{\varepsilon} \propto \sqrt{w_T}$. In this case the value of activation volume is less consistent with the value of γ obtained in the experiment. Thus, our semiquantitative analysis shows that the characteristics of the experimentally observed obtained processes in the plastic flow in ^{3}He can be treated in the framework of the mechanisms of dislocation motion in the Peierls relief. It seems that the case $\dot{\varepsilon} \propto w_T$ is realized. This experimentally determined activation energy E_a has a clear physical meaning: E_a equals twice the energy of a single kink.

As noted above, the experimentally observed independence of the velocity of plastic flow on temperature (Fig. 3) indicates the quantum mechanism of flow when at sufficiently low temperature the dislocation overcomes Peierls barriers by quantum tunneling. An estimate of the temperature T_0, below which the thermally activated regime of dislocation motion is replaced by the quantum tunneling, according to [20] gives $T_0 \approx 0.01$ K under mechanical stresses used in the experiment. Since the transition temperature to the athermal plasticity regime depends on the stress in the crystal, more accurate information can be obtained if we measure the dependence of the velocity of the plastic flow of helium on the mechanical stress in the quantum regime.

In conclusion, the quantum macroscopic plastic flow is observed for below 0.2 K. Earlier experiments on the plastic flow of solid ^{3}He were performed at temperatures above 0.5 K and only the classical thermally activated plastic flow was observed. It has been found that thermally activated flow regime is realized above $\sim$0.2 K, and the activation energy of the process is equal to the activation energy of vacancies. The activation volume 30–70 times exceeds the atomic volume, indicating that structural changes in the lattice during plastic

deformation occur on a scale considerably exceeding the atomic size. The results of experiment can be explained within the vacancy model if the sources of vacancies are areas with a high concentration of external stresses. The possible alternative explanation for the experimental data is based on the model of the motion of dislocations in the Peierls potential relief.

The authors thank V. D. Natsik, M. A. Strzhemechny, and S. S. Sokolov for useful discussions.

[1] E. Kim and M. H. W. Chan, Nature (London) **427**, 225 (2004).
[2] J. Beamish, Nature (London) **450**, 853 (2007).
[3] X. Rojas, A. Haziot, V. Bapst, S. Balibar, and H. J. Maris, Phys. Rev. Lett. **105**, 145302 (2010).
[4] John D. Reppy, Phys. Rev. Lett. **104**, 255301 (2010).
[5] A. Haziot, X. Rojas, A. D. Fefferman, J. R. Beamish, and S. Balibar, Phys. Rev. Lett. **110**, 035301 (2013).
[6] J. T. West, O. Syshchenko, J. Beamish, and M. H. W. Chan, Nat. Phys. **5**, 598 (2009).
[7] D. Y. Kim and M. H. W. Chan, Phys. Rev. Lett. **109**, 155301 (2012); Phys. Rev. B **90**, 064503 (2014).
[8] A. Sakai, Y. Nishioka, and H. Suzuki, J. Phys. Soc. Japn. **46**, 881 (1979).
[9] N. E. Dyumin, V. V. Boiko, N. V. Zuev, and V. N. Grigor'ev, Fiz. Nizk. Temp. **20**, 274 (1994) [Low Temp. Phys. **20**, 214 (1994)].
[10] N. E. Dyumin, V. V. Boiko, N. V. Zuev, and V. N. Grigor'ev, Fiz. Nizk. Temp. **21**, 509 (1995) [Low Temp. Phys. **21**, 395 (1995)]; N. V. Zuev, N. E. Dyumin, V. V. Boiko, and V. N. Grigor'ev, Fiz. Nizk. Temp. **22**, 215 (1996) [Low Temp. Phys. **22**, 167 (1996)].
[11] S. Balibar, J. Beamish, and R. B. Hallock, J. Low Temp. Phys. **180**, 3 (2015).
[12] V. A. Zhuchkov, A. A. Lisunov, V. A. Maidanov, A. S. Neoneta, V. Yu. Rubanskyi, S. P. Rubets, E. Ya. Rudavskii, and S. N. Smirnov, Low Temp. Phys. **41**, 169 (2015).
[13] J. P. Hirth and J. Lothe, *Theory of Dislocations* (McGraw-Hill, New York, 1968).
[14] S. M. Heald, D. R. Baer, and R. O. Simmons, Phys. Rev **30**, 2531 (1984).
[15] H. Neuber, *Kerbspannungslehre, Grundlagen für Genaue Spannungsrechnung* (Springer-Verlag, Berlin, 1937).
[16] D. M. Marsh, Philos. Mag. **5**, 1197 (1960).
[17] K. Schroder, J. Mech. Phys. Sol. **11**, 205 (1963).
[18] J. Friedel, *Dislocations* (Pergamon, New York, 1964).
[19] P. Guyot and J. E. Dorn, Can. J. Phys. **45**, 983 (1967).
[20] B. V. Petukhov and V. L. Pokrovskii, Zh. Eksp. Teor. Fiz. **63**, 634 (1972) [Sov. Phys. JETP **36**, 336 (1973)].
[21] A. Seeger, Zs. Metallkd. B **72**, 369 (1981).
[22] V. D. Natsik and X. J. Kaufmann, Phys. Status Solidi A **65**, 571 (1981).
[23] M. A. Strzhmechny, Fiz. Nizk. Temp. **10**, 663 (1984) [Sov. J. L. Temp. Phys. **10**, 348 (1984)].
[24] V. I. Nikitenko, *Dynamics of Dislocation* (Naukova Dumka, Kiev, 1975), pp. 7–26 (in Russian).
[25] G. I. Kirichenko, V. D. Natsik, and V. P. Soldatov, Fiz. Met. Metalloved **63**, 386 (1987) (in Russian).
[26] V. D. Natsik, G. I. Kirichenko, V. V. Pustovalov, V. P. Soldatov, and S. E. Shumilin, Fiz. Nizk. Temp. **22**, 965 (1996) [Low Temp. Phys. **22**, 740 (1996)].
[27] V. A. Moskalenko, V. D. Natsik, and V. N. Kovaleva, Low Temp. Phys. **31**, 907 (2005).
[28] A. Seeger, Z. Metallkd. **93**, 760 (2002).